

^{27}Al Solid-state Nuclear Magnetic Resonance Study of Five-Coordinate Aluminum in Augelite and Senegalite

William F. Bleam¹, Stephen F. Dec², and James S. Frye²

¹ University of Wisconsin-Madison, Madison, WI 53706, USA

² Department of Chemistry Colorado State University, Ft. Collins, CO 80523, USA

Abstract. This is a report of ^{27}Al magic-angle spinning, nuclear magnetic resonance spectroscopy of 5- and 6-coordinate aluminum in the aluminophosphate minerals *augelite* and *senegalite*. We have determined the quadrupolar coupling constants, asymmetry parameters and chemical shifts corrected for quadrupolar-induced shift for both aluminum coordination sites in each mineral. The quadrupolar coupling constants are significantly less in *senegalite* than in *augelite*. Structural analysis (viz., longitudinal- and shear-strain of the aluminum coordination polyhedra; coefficient-of-variation for both Al-O bond lengths and <O-Al-O bond angles) shows that both 5- and 6-coordinate aluminum sites in *senegalite* are less distorted than in *augelite*.

Introduction

The central nuclear magnetic resonance (NMR) transition of half-integer quadrupolar nuclei ($m_I = 1/2 \leftrightarrow m_I = -1/2$) is broadened, in part, by interaction between the nuclear quadrupolar moment and the electric field gradient at the nucleus. Unlike dipole-dipole interactions and chemical-shift anisotropy, the broadening caused by this interaction cannot be eliminated by magic-angle spinning (Andrew 1981). Second-order quadrupolar interactions can produce a complex powder pattern which depends on the spin quantum number, I , the quadrupolar coupling constant, e^2qQ/h , the asymmetry parameter, η , and the spinning angle (Narita et al. 1966; Nolle 1977; Müller et al. 1981; Kundla et al. 1981; Behrens and Schnabel 1982). The width of the second-order quadrupolar powder pattern, averaged by magic-angle spinning (MAS), is inversely proportional to the static magnetic field strength, B_0 (Meadows et al. 1982). This effect is the major source of the improvement in resolution with increasing B_0 for the spectra of half integer quadrupolar nuclides.

Quantitative NMR analysis of ^{27}Al ($I = 5/2$) is complicated by several factors. A commonly encountered problem is extreme width of the MAS-averaged second-order quadrupolar powder pattern causing overlap with other signals and spinning sidebands. This is common for e^2qQ/h greater than 8 MHz. A second source of quantitative error is loss of center-band ($m_I = 1/2 \leftrightarrow m_I = -1/2$) signal intensity into the spinning sideband array. The severity of this problem depends upon the static width of the signal arising from the central transition, which depends upon both e^2qQ/h

and the chemical shift anisotropy. Such intensity loss is generally ignored, and a correction procedure would often be complicated by the overlap of spinning sidebands arising from the non-central transitions (e.g., $m_I = 3/2 \leftrightarrow m_I = 1/2$). Ferric ions are a common contaminant in aluminum-containing samples, and these paramagnetic centers can broaden the signals of nearby ^{27}Al beyond detection. The broadening decreases with the sixth power of the inter-nuclear distance, so low concentrations of paramagnetic species are not likely to render an appreciable fraction of the ^{27}Al signal 'NMR invisible'.

^{27}Al signal loss (Bosacek et al. 1982), which can be as high as 95% (De Jong et al. 1983; MacKenzie et al. 1985), is commonly attributed to large quadrupolar coupling constants characteristic of coordination sites with non-cubic symmetry. Yet, Ghose and Tsang (1977) found low correlations between ^{27}Al quadrupolar coupling constants and two indices of coordination polyhedra distortion in aluminosilicates, "longitudinal strain" (viz., bond-length variation) or "shear strain" (viz., bond-angle variation).

The quadrupolar coupling constants for aluminum in 4-fold coordination are generally less than for 6-coordinate sites (Müller et al. 1981; Akitt and Farthing 1978; Lampe et al. 1982; Stade et al. 1984). Müller et al. (1983a) believe this is because 6-coordinate aluminum polyhedra are easier to distort than 4-coordinate polyhedra since Al-O bond lengths are larger in the former than in the latter. Recent results from minerals containing 5-coordinate aluminum (Cruickshank et al. 1986; Alemany and Kirker 1986; Lippmaa et al. 1986; Gilson et al. 1987; Alemany et al. 1988) illustrate the complex interplay between coordination number and site symmetry. 5-coordinate polyhedra would seem to be further from cubic symmetry than 4- or 6-coordinate sites in minerals, yet ^{27}Al spectra of 5-coordinate aluminum are readily observed in every study cited above. *Andalusite* is particularly intriguing in that the signal from the 5-coordinate aluminum dominates the spectra ($e^2qQ/h = 5.9$ MHz) while 6-coordinate aluminum ($e^2qQ/h = 15.6$ MHz) is difficult to detect (Alemany and Kirker 1986; Alemany et al. 1988). Even trends in e^2qQ/h cannot safely be predicted from qualitative symmetry arguments.

The aluminum in *augelite* (Araki et al. 1968), *senegalite* (Keegan et al. 1979) is evenly distributed over both 5- and 6-coordinate sites. This study reports the quadrupolar coupling constants and asymmetry parameters for the aluminum in these two minerals. We will also examine the rela-

Table 1. Aluminum phosphate minerals used in this study

Mineral	Identification	Empirical Formula	Space group
Augelite	NMNH # 137305	$\text{Al}_2(\text{OH})_3\text{PO}_4$	$C2/m$
Senegalite	NMNH # 137180	$\text{Al}_2(\text{OH})_3\text{PO}_4 \cdot \text{H}_2\text{O}$	$P2_1nb$

tion between the structure of *augelite* and *senegalite* and their ^{27}Al high-resolution NMR spectra.

Experimental Methods and Materials

^{27}Al spectra were collected on a Bruker AM-500 spectrometer (11.75 T) with a “homebuilt” magic-angle-spinning probe, ^{27}Al frequency = 130.3 MHz. A $\pi/2$ excitation pulse is 16 μs for 1M AlCl_3 (aq). Spinning rates of 12 to 13 kHz were attained using a Torlon rotor. Line broadening was 200 Hz. To verify that $T_{1\text{Al}}$ relaxation was not affecting relative signal intensities, we obtained spectra with both 0.004 and 250 ms delay times between repetitions.

The *augelite* (NMNH # 137305; Canada) and *senegalite* (NMNH # 137180; Senegal) samples were both naturally-occurring minerals (Table 1), provided by the Department of Mineral Sciences, National Museum of Natural History, Smithsonian Institution, Washington, DC.

Experimental Results

A typical single-pulse excitation, magic-angle spinning (MAS) spectrum of *augelite* appears in Fig. 1. Two distinct NMR powder patterns make up the spectrum. One extends from 30 to about 2 ppm, the second from 0 to -20 ppm. The “more shielded” pattern has the appearance characteristic of a coordination environment with asymmetry parameter, η , equal to zero (Nolle 1977; Kundla et al. 1981; Müller 1982; Samoson et al. 1982). The asymmetry parameter of the “less shielded” pattern is clearly non-zero (cf. Ganapathy et al. 1982).

Analysis of these MAS powder patterns using the technique of Müller (1982) and Samoson et al. (1982) yields the quadrupolar parameters appearing in Table 2. The parameters for the more shielded pattern were estimated using the two singularities at -3.1 and -10.9 ppm and the shoulder at -19.3 ppm, whose positions are all easily determined. Overlap of the two patterns forced us to use the maximum at 30 ppm, the two singularities at 17.2 and 15.1 ppm and the center-of-gravity at 17.2 ppm to estimate the parameters for the down-field pattern.

Coherence develops between the central and satellite transitions of half-integer quadrupolar nuclei during the non-resonance excitation pulse in a single-pulse excitation Fourier Transform NMR experiment (Samoson and Lippmaa 1983; Fenzke et al. 1984). If the excitation pulse length τ_p is less than $\pi/4\omega_{\text{rf}}(I+1/2)$, intensity of all signals will be proportional to τ_p and independent of the quadrupolar coupling constant. Our pulse lengths are below this limit. From integrated peak areas, neglecting spinning side-bands, the ratio of aluminum in the two sites is 1.0:1.0.

A MAS spectrum of *senegalite* appears in Fig. 2. As in *augelite*, two distinct NMR powder patterns make up the spectrum of *senegalite*. The two peaks at 124 and -57 ppm are spinning side bands of the peak with its center-of-gravity at 33.1 ppm, verified by MAS at different spinning

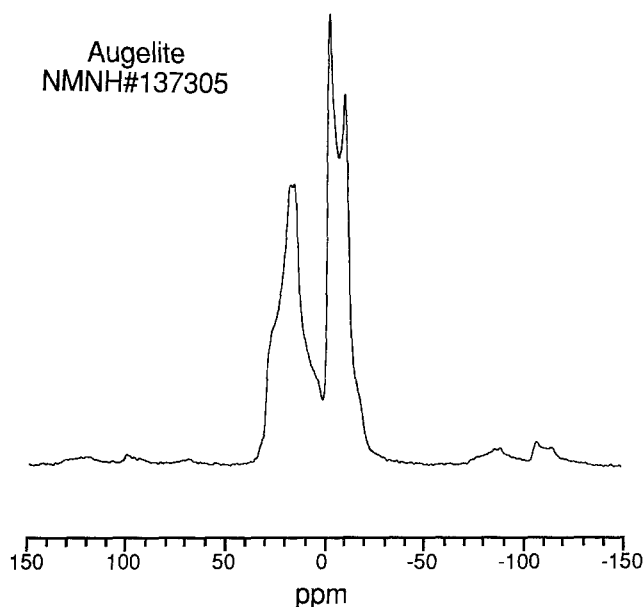


Fig. 1. 130.32 MHz ^{27}Al solid-state NMR spectra with 1 M AlCl_3 used as an external chemical shift reference. Augelite [NMNH # 137305] single-pulse excitation, MAS at 13.7 kHz spinning frequency: 200k scans, 1k data points, 125 kHz spectral width, 0.004 ms delay between repetitions, 0.5 μs pulse width

Table 2. Quadrupolar parameters for the mineral *augelite*

δ_{iso} , ppm	δ_{cog} , ppm ^a	$\Delta\delta$, ppm ^b	η	e^2qQ/h , MHz
30.9	17.2	14.0	0.85	5.7
0.3	-6.8	-7.1	1.00	4.5

^a center-of-gravity

^b quadrupolar-induced shift

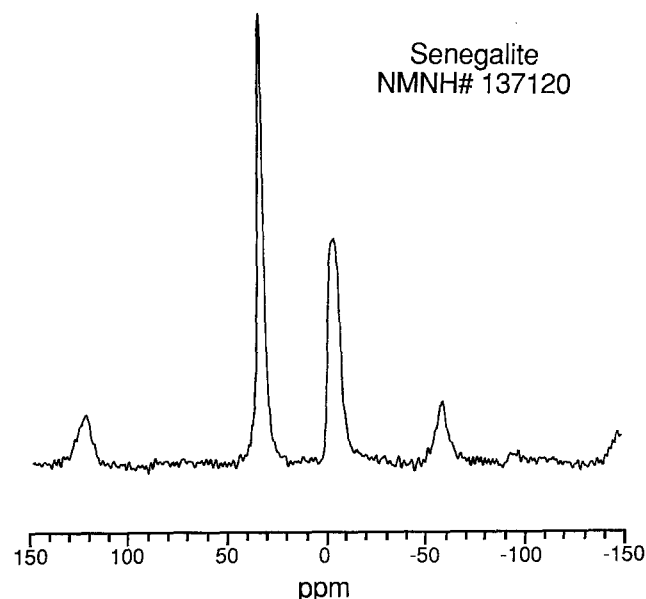


Fig. 2. 130.32 MHz ^{27}Al solid-state NMR spectra with 1 M AlCl_3 used as an external chemical shift reference. Senegalite [NMNH # 137180] single-pulse excitation, MAS at 11.7 kHz spinning frequency: 50k scans, 1k data points, 125 kHz spectral width, 0.004 ms delay between repetitions, 0.2 μs pulse width

Table 3. Quadrupolar parameters for the mineral *senegalite*

δ_{iso} , ppm	δ_{cog} , ppm ^a	$\Delta\delta$, ppm ^b	e^2qQ/h , MHz	
36.0	33.1	2.9	2.87 ^c	2.48 ^d
1.7	-6.8	-7.1	4.09 ^c	3.55 ^d

^a center-of-gravity^b quadrupolar-induced shift^c assuming: $\eta = 0$ ^d assuming: $\eta = 1$

frequencies. The small peak at -95 ppm is a spinning side band of the peak whose center-of-gravity is at -4.25 ppm. The absence of identifiable structure in the two central transitions in Figure 2 clearly show the quadrupolar coupling constants for the two coordination sites in *senegalite* are smaller than in *augelite*. We are unable to determine the asymmetry parameter since the peaks have a Gaussian shape. We estimated the quadrupolar-induced shift from the peak width at half-height (Freude et al. 1985). From the quadrupolar-induced shifts, we estimated the quadrupolar coupling constants (Müller 1982; Samoson et al. 1982). The quadrupolar parameters for *senegalite* appear in Table 3. Neglecting spinning side-bands, the integrated peak-area ratio, 33.1 ppm (center-of-gravity) to -4.25 (center-of-gravity), is 1.0:0.9.

Discussion

Quasi-trigonal bipyramidal coordination is evident in all of the 5-coordinate-containing aluminophosphates for which we have crystal structure refinements, viz. *augelite*, *senegalite* and $\text{AlPO}_4\text{-21}$ (Araki et al. 1968; Keegan et al. 1979; Bennett et al. 1985; Parise and Day, 1985). The mean Al-O bond lengths and mean bond angles for *augelite* and *senegalite* appear in Tables 4 and 5.

Although the coefficient of variation (standard deviation divided by the mean) for 5-coordinate aluminum bond lengths can be quite large, the mean bond lengths fall in a narrow range from 1.83 to 1.85 Å. In fact, they lie quite close to the average of the bond lengths typical for 4-coordinate and 6-coordinate aluminum, viz. 1.748 Å (Bailey 1980) and 1.909 Å (Brown and Shannon 1973) respectively. Table 4 clearly shows that the longitudinal strain, $|\alpha|$, and the coefficients-of-variation for Al-O bonds in both 5- and 6-coordinate sites are larger in *augelite* than in *senegalite*. Angular data shown in Table 5 tell the same tale. Distortion of aluminum coordination polyhedra, as indicated by these parameters, is significantly lower in *senegalite* compared to *augelite*, in agreement with the estimated relative quadrupolar coupling constants.

4-coordinate aluminum in AlPO_4 polymorphs, the aluminophosphate zeolite $\text{AlPO}_4\text{-5}$, and calcium aluminum phosphate glasses (Müller et al. 1983a; Müller et al. 1983b; Blackwell and Patton 1984; Müller et al. 1985; Nakata et al. 1986) give rise to chemical shifts in the range of $+37$ to $+44$ ppm relative to $\text{Al}(\text{H}_2\text{O})_6^{3+}$. Müller et al. (1983a) found that 6-coordinate aluminum in calcium aluminum phosphate glasses resonates at -15 to -21 ppm. The range is about the same for crystalline aluminum phosphates (Müller et al. 1983b; Blackwell and Patton 1984). These shifts, and those for 4-coordinate aluminum, are about 30 ppm more shielded than aluminas and aluminosilicates.

Table 4. Mean aluminum-oxygen bond lengths, $l_{\text{Al-O}}$, coefficients of bond-length variation, and longitudinal strain, $|\alpha|^a$, for 5- and 6-coordinate aluminum in *augelite* and *senegalite*

Mineral	$l_{\text{Al-O}}^b$, Å		$l_{\text{Al-O}}^c$, Å		$ \alpha_s $	$ \alpha_e $
<i>Augelite</i>	1.832	0.068 ^d	1.891	0.039 ^d	0.238	0.194
<i>Senegalite</i>	1.848	0.031 ^d	1.899	0.029 ^d	0.120	0.067

^a longitudinal strain, $|\alpha| = \sum_i |\ln(l_i/l_{\text{mean}})|$ (Ghose and Tsang 1977)^b 5-coordinate^c 6-coordinate^d coefficient-of-variation, standard deviation divided by mean bond length**Table 5.** Shear strain, $|\psi|^a$, mean oxygen-aluminum-oxygen bond angles, and coefficients of bond-angle variation 5- and 6-coordinate aluminum in *augelite* and *senegalite*

Shear Strain	$ \psi_s $		$ \psi_e $	
<i>Augelite</i>	1.382	0.623	1.464	0.787
<i>Senegalite</i>	0.623	0.787	0.787	0.623

Bond Angles ^b	axial	equatorial	axial-equatorial	
<i>Augelite</i>	170.0°	118.2°	0.067 ^c	89.9°
<i>Senegalite</i>	172.5°	119.7°	0.049 ^c	90.0°

^a shear strain, $|\psi| = \sum_i |\tan(\theta_i - \theta_{\text{ideal}})|$ (Ghose and Tsang 1977)^b 5-coordinate sites only^c coefficient-of-variation, standard deviation divided by the mean bond angle

Alemany et al. (1988) found a chemical shift range of 14 to 16 ppm for 5-coordinate aluminum in $\text{AlPO}_4\text{-21}$. The shift of 5-coordinate aluminum in phosphates relative to oxides is between 35 to 45 ppm toward greater shielding (Lippmaa et al. 1986; Cruickshank et al. 1986; Alemany and Kirker 1986). We should note that chemical shifts reported in the literature are not always corrected for quadrupolar-induced shifts.

We assign the $\delta_{\text{iso}} = 0.3$ ppm resonance in *augelite* and the $\delta_{\text{iso}} = 1.7$ ppm resonance in *senegalite* to aluminum in 6-coordinate sites. The remaining resonance, $\delta_{\text{iso}} = 30.9$ ppm in *augelite* and $\delta_{\text{iso}} = 36.0$ ppm in *senegalite*, are assigned to 5-coordinate aluminum. We make these assignments on the basis of relative peak positions, the chemical shift of 6-coordinate aluminum and the mineral structure (Lippmaa et al. 1986; Cruickshank et al. 1986; Alemany et al. 1988). Interestingly, *augelite* and *senegalite* do not exhibit the 30 ppm shift toward increased shielding observed for other aluminophosphates (Müller et al. 1983b; Alemany et al. 1988).

While longitudinal-strain, shear-strain and coefficients-of-variation in either bond length or bond-angle cannot fully express the electric field gradient, the qualitative observation that aluminum coordination polyhedra are less distorted in *senegalite* than *augelite* is borne out in the quadrupolar coupling constants for the two minerals.

Acknowledgements. The Colorado State University Regional NMR Center is funded by National Science Foundation Grant No. CHE-8616437. W.F.B. wishes to thank Peter Dunn of the Department of Mineral Sciences, Natural Museum of Natural History-Smith-

sonian Institution, Washington, DC who generously provided the *augelite* and *senegalite* samples.

References

- Akitt JW, Farthing A (1978) New ^{27}Al NMR studies of the hydrolysis of the aluminum (III) cation. *J Magn Reson* 32:345–352
- Aleman LB, Kirker GW (1986) First observation of 5-coordinate aluminum by MAS ^{27}Al NMR in well-characterized solids. *J Am Chem Soc* 108:6158–6162
- Aleman LB, Timken HKC, Johnson ID (1988) Aluminum-27 NMR study of $\text{AlPO}_4\text{-21}$ and andalusite. Advantages of high-field and very fast MAS. *J Magn Reson* 80:427–438
- Andrew ER (1981) Magic angle spinning. *Int Rev Phys Chem* 1:195–224
- Araki T, Finney JJ, Zoltai T (1968) The crystal structure of *augelite*. *Am Mineral* 53:1096–1103
- Bailey SW (1980) Structures of layer silicates. In: Brindley GW, Brown G (eds) *Crystal structures of clay minerals and their x-ray identification*, Mineralogical Society, London, pp 1–124
- Behrens H-J, Schnabel B (1982) The second order influence of the nuclear quadrupole interaction on the central line in the NMR of quadrupolar nuclei using rapid sample spinning. *Physica B* 114:185–190
- Bennett JM, Cohen JM, Artioli G, Pluth JJ, Smith JV (1985) Crystal structure of $\text{AlPO}_4\text{-21}$, a framework aluminophosphate containing tetrahedral phosphorus and both tetrahedral and trigonal-bipyramidal aluminum in 3-, 4-, 5- and 8-rings. *Inorg Chem* 24:181–193
- Blackwell CC, Patton RL (1984) Aluminum-27 and phosphorus-31 nuclear magnetic resonance studies of aluminophosphate molecular sieves. *J Phys Chem* 88:6135–6139
- Bosacek V, Freude D, Fröhlich T, Pfeifer H, Schmiedel H (1982) NMR studies of ^{27}Al in decationated Y zeolite. *J Colloid Interface Sci* 85:502–507
- Brown ID, Shannon RD (1973) Empirical bond-strength-bond-length curves for oxides. *Acta Crystallogr A* 29:266–282
- Cruickshank MC, Glasser LSD, Barri SAI, Poplett IJF (1986) Penta-co-ordinated aluminium: A solid-state ^{27}Al NMR study. *J Chem Soc Chem Commun* 88:23–24
- De Jong BHWS, Schramm CM, Parziale VE (1983) Polymerization of silicate and aluminate tetrahedra in glasses, melts, and aqueous solutions – IV. Aluminum coordination in glasses and aqueous solutions and comments on the aluminum avoidance principle. *Geochim Cosmochim Acta* 47:1223–1236
- Fenzke D, Freude D, Fröhlich T, Haase J (1984) NMR intensity measurements of half-integer quadrupolar nuclei. *Chem Phys Lett* 111:171–175
- Freude D, Haase J, Klinowski J, Carpenter TA, Ronikier G (1985) NMR line shifts caused by the second-order quadrupolar interaction. *Chem Phys Lett* 119:365–367
- Ghose S, Tsang T (1977) Structural dependence of quadrupole coupling constant e^2qQ/h for ^{27}Al and crystal field parameter D for Fe^{3+} in aluminosilicates. *Am Mineral* 58:748–755
- Gilson JP, Edwards GC, Peters AW, Rajagopalan K, Wormsbecher RF, Roberie TG, Shatlock MP (1987) Penta-co-ordinated aluminium in zeolites and aluminosilicates. *J Chem Soc Chem Commun* pp 91–92
- Keegan TD, Araki T, Moore PB (1979) *Senegalite*, $\text{Al}_2(\text{OH})_3\text{-(H}_2\text{O)}(\text{PO}_4)$, a novel structure type. *Am Mineral* 64:1243–1247
- Kundla E, Samoson A, Lippmaa E (1981) High-resolution NMR of quadrupolar nuclei in rotating solids. *Chem Phys Lett* 83:229–232
- Lampe VL, Müller D, Gessner W, Grimmer AR, Scheler G (1982) Vergleichende ^{27}Al -NMR-Untersuchungen am Mineral *Zunytit* und basischen Aluminium-Salzen mit tridentameren Al-oxo-hydroxo-aquo-Kationen. *Z Anorg Allg Chem* 489:16–22
- Lippmaa E, Samoson A, Mägi M (1986) High resolution ^{27}Al NMR of aluminosilicates. *J Am Chem Soc* 108:1730–1735
- MacKenzie KJD, Brown IWM, Meinhold RH, Bowden ME (1985) Thermal reactions of pyrophyllite studied by high-resolution solid-state ^{29}Si and ^{27}Al nuclear magnetic resonance spectroscopy. *J Am Ceram Soc* 68:266–272
- Meadows MD, Smith KA, Kinsey RA, Rothgeb TM, Skarjune RP, Oldfield E (1982) High-resolution solid-state NMR of quadrupolar nuclei. *Proc Natl Acad Sci* 79:1351–1355
- Müller D (1982) Zur Bestimmung chemischer Verschiebungen der NMR-Frequenzen bei quadrupolkernen aus den MAS-NMR-Spektren. *Ann Phys* 7:451–460
- Müller D, Gessner W, Behrens H-J, Scheler G (1981) Determination of the aluminum coordination in aluminum-oxygen compounds by solid-state high-resolution ^{27}Al NMR. *Chem Phys Lett* 79:59–62
- Müller D, Berger G, Grunze I, Ladwig G, Hallas E, Haubenreisser U (1983a) Solid-state high-resolution ^{27}Al nuclear magnetic resonance studies of the structure of $\text{CaO-Al}_2\text{O}_3\text{-P}_2\text{O}_5$ glasses. *Phys Chem Glasses* 24:37–42
- Müller D, Grunze I, Hallas E, Ladwig G (1983b) Hochfeld- ^{27}Al -NMR Untersuchungen zur Aluminiumkoordination in kristallinen Aluminiumphosphaten. *Z Anorg Allg Chem* 500:80–83
- Müller D, Jahn E, Fahlke B, Ladwig G, Haubenreisser U (1985) High resolution ^{27}Al and ^{31}P n.m.r. studies of the aluminum phosphate molecular sieve $\text{AlPO}_4\text{-5}$. *Zeolites* 5:53–56
- Narita K, Umeda J-I, Kusumoto H (1966) Nuclear magnetic resonance powder patterns of the second-order nuclear quadrupole interaction in solids with asymmetric field gradients. *J Chem Phys* 44:2719–2723
- Nataka S-I, Asaoka S, Takahashi H, Deguchi K (1986) High-resolution solid-state phosphorus-31 MASNMR studies of inorganic phosphates. *Anal Sci* 2:91–93
- Nolle A (1977) Second-order quadrupolar splittings of the ^{95}Mo NMR signal in $\text{Mo}(\text{CO})_6$ and their reduction by sample spinning. *Z Phys A-Atoms and Nuclei* 280:231–234
- Parise JB, Day CS (1985) The structure of trialuminum tris(orthophosphate) Hydrate, $\text{AlPO}_4\text{-21}$, with clathrated ethylenediamine, $\text{Al}_3(\text{PO}_4)_3 \cdot \text{C}_2\text{H}_8\text{N}_2 \cdot \text{H}_2\text{O}$, and pyrrolidine, $\text{Al}_3(\text{PO}_4)_3 \cdot \text{C}_4\text{H}_9\text{N} \cdot \text{H}_2\text{O}$. *Acta Crystallogr C* 41:515–520
- Samoson A, Lippmaa E (1983) Excitation phenomena and line intensities in high-resolution NMR powder spectra of half-integer quadrupolar nuclei. *Phys Rev B* 28:6567–6570
- Stade H, Müller D, Scheler G (1984) ^{27}Al -NMR-spektroskopische Untersuchungen zur Koordination des Al in C-S-H(Di, Poly). *Z Anorg Allg Chem* 510:16–24

Received June 12, 1989